

The asymmetric simple exclusion process on chains with a shortcut revisited

Nadezhda Bunzarova^{1,2}, Nina Pesheva², and Jordan Brankov^{1,2}

¹ *Bogoliubov Laboratory of Theoretical Physics,*

Joint Institute for Nuclear Research, 141980 Dubna, Russian Federation

² *Institute of Mechanics, Bulgarian Academy of Sciences, 1113 Sofia, Bulgaria*

We consider the asymmetric simple exclusion process (TASEP) on open network consisting of three consecutively coupled macroscopic chain segments with a shortcut between the tail of the first segment and the head of the third one. The model was introduced by Y.-M. Yuan et al [J. Phys. A 40, 12351 (2007)] to describe directed motion of molecular motors along filaments. We report here unexpected results in the case of maximum current through the network which revise the previous findings. Our theoretical analysis, based on the effective rates approximation, shows that the second (shunted) segment can exist in both low-density and high-density phases, as well as in the coexistence (shock) phase. Numerical simulations demonstrate that it is the last option that takes place - the local density distribution and the nearest-neighbor correlations in the middle chain correspond to a shock phase with completely delocalized domain wall. Surprisingly, the main quantitative parameters of that shock phase are governed by a real root of a cubic equation the coefficients of which simply depend on the probability of choosing the shortcut. The unexpected conclusion is that a shortcut in the bulk of a single lane always creates traffic jams.

Pacs: 02.50.Ey, 05.60.-k, 05.70.Ln

Keywords: TASEP, traffic flow models, non-equilibrium phase transitions, traffic on complex networks, biological transport

Introduction. — The asymmetric simple exclusion process (TASEP) is one of the paradigmatic models for understanding the rich world of non-equilibrium phenomena. Devised to model kinetics of protein synthesis [1], it has found a number of applications to vehicular traffic flow [2], biological transport [3], one-dimensional surface growth [4], forced motion of colloids in narrow channels [5], spintronics [7], transport of 'data packets' in the Internet [6], current through chains of quantum dots [8], to mention some.

Novel features of the TASEP have been found on networks consisting of coupled linear chains with nontrivial geometry. In the approach advanced in our work [9] each macroscopic segment s of the network is considered in a stationary phase determined by its effective injection α_s^* and ejection β_s^* rates. At that, exact in the thermodynamic limit results for the density profile are incorporated. The only molecular field type approximation used consists in the neglect of correlations between different chain segments. This allows one to treat the coupling between each two connected segments as coupling to reservoirs with certain effective rates. The possible phase structures of the whole network are obtained as solutions of the resulting set of equations for the effective rates that follow from continuity of current. The importance of our approach for modeling complex biological transport phenomena was pointed out by Pronina and Kolomeisky [10]. This method became very popular and was used in a number of studies of TASEP and its generalizations on networks with different geometries, e.g., with junctions, bifurcations, intersections, interacting lanes [11]. Finite-size effects on the density profile due to shifting the position of the double-chain section from the middle of the linear network were studied too [12].

Here we consider the TASEP on open chain with a shortcut in the bulk, introduced as 'model A' in [13]. The current through the shortcut is proportional to a probability q . It is convenient to consider the system as composed of three consecutively connected macroscopic chain segments and a shortcut between the tail of the first segment and the head of the third one. In principle, the effect of a shortcut can easily be understood: the decrease in the current through the shunted part (second segment) of the original chain leads to a sharp change of the particle density in the latter. If the chain without a shortcut ($q = 0$) is in the low-density (LD) phase, its bulk density $\rho_{\text{bulk}}^{\text{LD}} < 1/2$ supports a current $J = \rho_{\text{bulk}}^{\text{LD}}(1 - \rho_{\text{bulk}}^{\text{LD}}) < 1/4$. The shortcut takes a part $J^{\text{sc}} > 0$ of that current away from the second segment, hence the current $J^{(2)} = J - J^{\text{sc}}$ has to be supported by still less bulk density $\rho_{\text{bulk}}^{(2)} < \rho_{\text{bulk}}^{\text{LD}}$ in that segment. Similarly, when the initial chain is in the high-density

(HD) phase with $\rho_{\text{bulk}}^{\text{HD}} > 1/2$, the drop in the current through the second segment, caused by the shortcut, leads to a still higher bulk density in that segment, $\rho_{\text{bulk}}^{(2)} > \rho_{\text{bulk}}^{\text{HD}}$. In these cases all the three segments remain in the same phase, though with different density of the middle one.

Not so clear, however, is the situation when the initial chain is in the maximum current (MC) phase with $\rho_{\text{bulk}}^{\text{MC}} = 1/2$. Now the drop in the current through the shunted segment of the network can be compensated equally well by decrease or increase in its bulk density. Then, the middle segment is forced either in low-density, or in high-density phase, which may lead also to coexistence of LD phase on the left-hand side with HD phase on the right-hand side. This phase structure is additionally favored by the downward (upward) bend in the density profile of the first (third) segment in the maximum current phase. In the case of open system with variable total number of particles the coexisting phases are likely to be separated by a completely delocalized domain wall. Such was the situation observed in each of the equivalent segments in a double-chain section incorporated in the middle of a long linear chain [9]. It seems plausible that the above mechanism of influence of the shortcut on the phase state of the shunted segment should be invariant with respect to the explicit structure of the shortcut. In particular, one may consider a shortcut in the form of an additional (shorter) chain connecting the last site of the first segment to the first site of the third one. Since the length of the shortcut is irrelevant, we can include the case of parallel segments with equal length considered in our work [9]. However, the authors of [13] have claimed that in the case of their 'model A', the shunted middle segment can exist only in the high-density phase. This contrast in the conclusions motivated us to renew the study, both analytically and numerically, of the model. The results may have important implications for vehicular traffic flow control, as well as for biological transport in living cells.

Microscopic model. — Here we consider model A of a shortcut, suggested in [13], when both the injection α and ejection β rates at the open ends of the system are larger than $1/2$, so that the first and third segments are in the maximum current phase. The shortcut is between the last site of the first segment, with occupation number $\tau_L^{(1)}$, and the first site of the third segment, with occupation number $\tau_1^{(3)}$. According the rules of the random-sequential algorithm, when a particle at the last site of the first segment (with $\tau_L^{(1)} = 1$) attempts to move, the particle may jump along the main track to the first site of the second segment with rate $(1-q)(1-\tau_1^{(2)})(1-\tau_1^{(3)}) + (1-\tau_1^{(2)})\tau_1^{(3)}$, or take the shortcut to the first site of the

third segment with rate $q(1 - \tau_1^{(3)})$, or stay immobile with rate $(1 - q)\tau_1^{(2)}(1 - \tau_1^{(3)}) + \tau_1^{(2)}\tau_1^{(3)}$. These rules lead to exact expressions for the stationary current through segment 2,

$$J^{(2)} = (1 - q)\langle \tau_L^{(1)}(1 - \tau_1^{(2)})(1 - \tau_1^{(3)}) \rangle + \langle \tau_L^{(1)}(1 - \tau_1^{(2)})\tau_1^{(3)} \rangle = \langle \tau_L^{(2)}(1 - \tau_1^{(3)}) \rangle, \quad (1)$$

and through the shortcut $J^{\text{sc}} = q\langle \tau_L^{(1)}(1 - \tau_1^{(3)}) \rangle$, $0 \leq q \leq 1$.

Theoretical analysis. — In the effective rates analysis [9] one neglects the correlations between sites belonging to different segments, so that the above expressions simplify to

$$J^{(2)} = \rho_L^{(1)}(1 - \rho_1^{(2)})[(1 - q)(1 - \rho_1^{(3)}) + \rho_1^{(3)}] = \rho_L^{(2)}(1 - \rho_1^{(3)}), \quad (2)$$

and $J^{\text{sc}} = q\rho_L^{(1)}(1 - \rho_1^{(3)})$, where $\rho_i^{(s)} = \langle \tau_i^{(s)} \rangle$, $s = 1, 2, 3$, is the average value of the occupation number $\tau_i^{(s)}$ in a given stationary state. Within the above approximation effective injection, α_s^* , and ejection, β_s^* , rates for segment $s = 1, 2, 3$ are introduced according to the rule [9] $J^{(s)} = \beta_s^*\rho_L^{(s)} = \alpha_s^*(1 - \rho_1^{(s)})$, with $\alpha_1^* = \alpha$ and $\beta_3^* = \beta$. Thus, taking into account that $J^{(1)} = J^{(3)} = J^{(2)} + J^{\text{sc}}$, one obtains

$$\alpha_1^* = \alpha, \quad \beta_1^* = 1 - \rho_1^{(2)} + q\rho_1^{(2)}(1 - \rho_1^{(3)}), \quad (3)$$

$$\alpha_2^* = \rho_L^{(1)}[1 - q(1 - \rho_1^{(3)})], \quad \beta_2^* = 1 - \rho_1^{(3)}, \quad (4)$$

$$\alpha_3^* = \rho_L^{(2)} + q\rho_L^{(1)}, \quad \beta_3^* = \beta. \quad (5)$$

Here we have taken into account that α_3^* comes from both the expression for the current J^{sc} and the last one in (2). Expressions (3)-(5) for the effective rates coincide exactly with equations (4) obtained in [13]. However, the results of our analysis in the case when the first and third segments are in the maximum current phase are essentially different from those claimed in [13].

We confine ourselves to the study of possible phase structures of the type (M, X, M) , when the first and third segments are in the maximum current phase M , and the second segment is in a low-density phase ($X = L$), high-density one ($X = H$), or on the coexistence line ($X = C$). Note that the case ($X = M$) is excluded, since the presence of a shortcut ($J^{\text{sc}} > 0$) implies $J^{(2)} < J^{(1)} = J^{(3)} = 1/4$. To check the consistency of a given structure (M, X, M) with the corresponding conditions on the effective rates (3)-(5), we make use of the known, exact in the thermodynamic limit, values of the bulk density $\rho_{\text{bulk}}^{(s)}$ and local densities $\rho_1^{(s)}, \rho_L^{(s)}$, in dependance on the thermodynamic phase of each segment $s = 1, 2, 3$

[14]. At that we assume that all the segments have an equal, large enough length $L \gg 1$. Thus, in all cases under consideration one has

$$\rho_{\text{bulk}}^{(1)} = 1/2, \quad \rho_1^{(1)} = 1 - 1/(4\alpha), \quad \rho_L^{(1)} = 1/(4\beta_1^*) \quad (6)$$

$$\rho_{\text{bulk}}^{(3)} = 1/2, \quad \rho_1^{(3)} = 1 - 1/(4\alpha_3^*), \quad \rho_L^{(3)} = 1/(4\beta). \quad (7)$$

By inserting the expressions for $\rho_L^{(1)}$ and $\rho_1^{(3)}$ into Eq. (4), we obtain

$$\alpha_2^* = 1/(4\beta_1^*) - q/(16\alpha_3^*\beta_1^*), \quad \beta_2^* = 1/(4\alpha_3^*), \quad (8)$$

and, from Eq. (2), $J^{\text{sc}} = 1/4 - J^{(2)} = q/(16\beta_1^*\alpha_3^*)$. Now we pass to the separate consideration of each of the possibilities $X = L, H, C$.

Middle segment in the low-density phase. — In this case

$$\rho_{\text{bulk}}^{(2)} = \rho_1^{(2)} = \alpha_2^*, \quad J^{(2)} = \alpha_2^*(1 - \alpha_2^*), \quad \rho_L^{(2)} = \alpha_2^*(1 - \alpha_2^*)/\beta_2^*. \quad (9)$$

Substituting the expressions for $\rho_1^{(2)}$ and $\rho_L^{(2)}$ into Eqs. (3) and (5), we find

$$\beta_1^* = 1 - \alpha_2^*[1 - q/(4\alpha_3^*)], \quad \alpha_3^* = \alpha_2^*(1 - \alpha_2^*)/\beta_2^* + q/(4\beta_1^*). \quad (10)$$

We have obtained a set of four nonlinear equations, see (8) and (10), for the four effective rates β_1^* , α_2^* , β_2^* , and α_3^* . The solution depends on one free parameter, because one of these equations is a consequence of the other three. From the first equation in (8), we obtain the equation $\alpha_2^* = 1/(4\beta_1^*) - J^{\text{sc}} = 1/(4\beta_1^*) - 1/4 + \alpha_2^*(1 - \alpha_2^*)$, where we have used the relationship $J^{\text{sc}} = 1/4 - J^{(2)}$ in combination with the expression for $J^{(2)}$ given in (9). Hence, we find $\beta_1^* = 1/[1 + 4(\alpha_2^*)^2]$. After substitution of this expression into the first equation (10), we solve the latter for α_3^* and obtain $\alpha_3^* = q[1 + 4(\alpha_2^*)^2]/[4(1 - 2\alpha_2^*)^2]$. Finally, the second equation in (8) yields $\beta_2^* = (1 - 2\alpha_2^*)^2/\{q[1 + 4(\alpha_2^*)^2]\}$. Now one can readily verify that the above expressions for β_1^* , α_3^* and β_2^* identically satisfy the second equation in (10).

It remains to check the consistence of the results obtained with the conditions for (M, L, M) phase structure of the network. The free parameter α_2^* has to satisfy the inequality $\alpha_2^* < 1/2$ which is necessary for the second segment to be in low-density phase. The latter inequality implies $\beta_1^* > 1/2$ which, together with $\alpha > 1/2$ ensures that the first segment is in the maximum current phase. The remaining condition $\alpha_2^* < \beta_2^*$ for the second segment to be in the low-density phase leads to the cubic inequality

$$4q(\alpha_2^*)^3 - 4(\alpha_2^*)^2 + (4 + q)\alpha_2^* - 1 < 0. \quad (11)$$

This inequality has to be fulfilled simultaneously with the condition $\alpha_3^* > 1/2$ for the third segment to be in the maximum current phase (given $\beta > 1/2$), which implies $(1 - 2\alpha_2^*)^2 < (q/2)[1 + 4(\alpha_2^*)^2]$. Therefore, the free parameter α_2^* has to obey the constraints

$$q\alpha_2^*[1 + 4(\alpha_2^*)^2] < (1 - 2\alpha_2^*)^2 < (q/2)[1 + 4(\alpha_2^*)^2] \quad (12)$$

which define a nonempty interval when $\alpha_2^* < 1/2$. As a simple consequence, in the case of vanishing probability of the shortcut, $q \rightarrow 0^-$, the free parameter $\alpha_2^* \rightarrow 1/2^-$, which agrees with the result $\alpha_2^* = \rho_{\text{bulk}} = 1/2$ for a single chain in the maximum current phase.

Middle segment in the high-density phase. — In this case the exact thermodynamic parameters of the second segment are

$$\rho_{\text{bulk}}^{(2)} = \rho_L^{(2)} = 1 - \beta_2^*, \quad J^{(2)} = \beta_2^*(1 - \beta_2^*), \quad \rho_1^{(2)} = 1 - \beta_2^*(1 - \beta_2^*)/\alpha_2^*. \quad (13)$$

Substituting the above expressions for $\rho_1^{(2)}$ and $\rho_L^{(2)}$ into Eqs. (3) and (5), we find

$$\beta_1^* = q/(4\alpha_3^*) + [1 - q/(4\alpha_3^*)]\beta_2^*(1 - \beta_2^*)/\alpha_2^*, \quad \alpha_3^* = 1 - \beta_2^* + q/(4\beta_1^*). \quad (14)$$

Taking into account Eqs. (8), we have again a set of four nonlinear equations for the four effective rates. We shall solve these equations and show that one of them is a consequence of the other three. As in the previous case, one of the effective rates will appear as a free parameter in the solution. The second equation in (8) yields $\alpha_3^* = 1/(4\beta_2^*)$. Combining this result with the second equation in (14), we express β_1^* as a function of β_2^* : $\beta_1^* = q\beta_2^*/[1 - 4\beta_2^*(1 - \beta_2^*)]$. Taking into account that the current through the shortcut is $J^{\text{sc}} = 1/4 - J^{(2)}$, in view of the present expression for the current $J^{(2)}$, see Eq. (13), we can rewrite the first equation in (8) as $\alpha_2^* = 1/(4\beta_1^*) - 1/4 + \beta_2^*(1 - \beta_2^*)$. The substitution here of β_1^* yields $\alpha_2^* = [1/(q\beta_2^*) - 1][1/4 - \beta_2^*(1 - \beta_2^*)]$. One can readily check that the above expressions for α_2^* , α_3^* , and β_1^* satisfy the first equation in (14) identically with respect to $\beta_2^* = 1 - \rho_L^{(2)}$.

Finally, we check the conditions on the effective rates which imply the phase structure (M, H, M) . The condition $\alpha_2^* > \beta_2^*$ leads to the cubic inequality

$$4q(\beta_2^*)^3 - 4(\beta_2^*)^2 + (4 + q)\beta_2^* - 1 > 0, \quad (15)$$

which, together with $\beta_2^* < 1/2$ ensures the high-density phase of the second segment. The first segment is in the maximum current phase when $\alpha > 1/2$ and $\beta_1^* > 1/2$. The second condition leads to the inequality $q\beta_2^* > (1/2)[1 - 4\beta_2^*(1 - \beta_2^*)]$. The right-hand side being

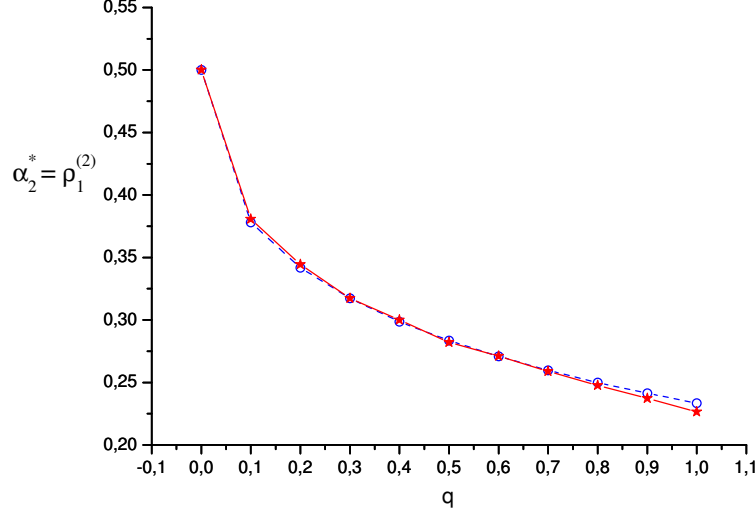


FIG. 1. (Color online) Comparison of the numerically evaluated $a_2^* = \rho_1^{(2)}$, shown by red stars, with the values of the appropriate root of the cubic equation (18), shown by blue circles, for ten different values of the rate q .

non-negative, $q \rightarrow 0$ implies $\beta_2^* \rightarrow 1/2$, hence $J^{(2)} \rightarrow 1/4$ and $J^{\text{sc}} \rightarrow 0$. The analysis of this quadratic inequality is equivalent to $\beta_2^* < 1/2 + q/4 - (1/4)\sqrt{q(4+q)}$, the right-hand side of which is less than $1/2$. The condition $\alpha_3^* > 1/2$ for the third segment to be in the maximum current phase (given $\beta > 1/2$) is satisfied whenever $\beta_2^* < 1/2$.

Middle segment on the coexistence line. — The second segment can exist in a low- or high-density phase, depending on whether $\alpha_2^* > \beta_2^*$ or $\alpha_2^* < \beta_2^*$, respectively. Naturally, we expect the coexistence phase (shock phase) to take place at a common point in the closure of the above open sets, i.e., when the rates $\alpha_2^* = \beta_2^*$ coincide with an appropriate root of the cubic equation given by an equality sign in expressions (15) and (11). To prove this, we set $\alpha_2^* = \beta_2^*$ and assume the exact in the thermodynamic limit values of the current and the local densities at the endpoints of the second segment in the coexistence phase,

$$J^{(2)} = \alpha_2^*(1 - \alpha_2^*) = \beta_2^*(1 - \beta_2^*), \quad \rho_1^{(2)} = \alpha_2^* = \rho_-(J^{(2)}), \quad \rho_L^{(2)} = 1 - \alpha_2^* = \rho_+(J^{(2)}). \quad (16)$$

Here $\rho_{\pm}(J) = (1 \pm \sqrt{1 - 4J})/2$ are the bulk densities in the high- and low-density phase, respectively, of a single chain with a current J . Substituting the above expressions for $\rho_1^{(2)}$ and $\rho_L^{(2)}$ into Eqs. (3) and (5), we obtain

$$\beta_1^* = \rho_+(J^{(2)}) + q\rho_+(J^{(2)})/(4\alpha_3^*), \quad \alpha_3^* = \rho_+(J^{(2)}) + q/(4\beta_1^*). \quad (17)$$

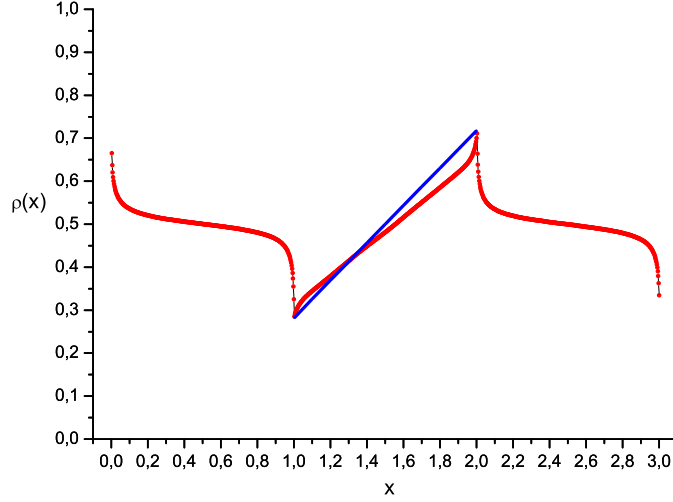


FIG. 2. (Color online) Local density profile at $\alpha = \beta = 0.75$ and $q = 0.5$ shown by red stars as a function of the normalized coordinate $x = i/L$, where $i = (s - 1)L + 1, (s - 1)L + 2, \dots, sL$ labels the sites in the segment s , $s = 1, 2, 3$. The shape of the density profile in the first and third segments is typical for the MC phase, while that in the second segment closely resembles the linear dependence with the distance characteristic of the coexistence phase with completely delocalized domain wall. The predictions of the domain wall theory are shown by a blue line.

Inserting in the first equation $1/(4\alpha_3^*)$ expressed from the second equation in (8) with $\beta_2^* = \alpha_2^*$, and replacing $\rho_+(J^{(2)})$ and $\rho_-(J^{(2)})$ by $1 - \alpha_2^*$ and α_2^* , respectively, we obtain $\beta_1^* = 1 - \alpha_2^* + q(\alpha_2^*)^2$. On the other hand, dividing both sides of the first equation in (17) by $4\beta_1^*$, and using $J^{\text{sc}} = 1/4 - J^{(2)}$, we arrive at $1/4 = \rho_+(J^{(2)})/(4\beta_1^*) + \rho_-(J^{(2)}) (1/4 - J^{(2)})$. Solving the above for β_1^* , and using that $J^{(2)} = \rho_+(J^{(2)})\rho_-(J^{(2)}) = \rho_+(J^{(2)})\alpha_2^*$, we obtain $\beta_1^* = [1 + 4(\alpha_2^*)^2]^{-1}$. Clearly, $\beta_1^* > 1/2$ when $\alpha_2^* < 1/2$. The equality the right-hand sides of the two above derived expressions for β_1^* leads to the equation

$$4q(\alpha_2^*)^3 - 4(\alpha_2^*)^2 + (4 + q)\alpha_2^* - 1 = 0. \quad (18)$$

Unexpectedly, the value of $\alpha_2^* = \beta_2^*$ is determined by a root of cubic equation, which is singular at $q = 0$. More precisely, these effective rates are given as function of q , $0 \leq q \leq 1$, by the real root of Eq. (18) which is less than $1/2$ and tends to $1/2$ from below as $q \rightarrow 0^+$. A comparison of the values of α_2^* given by the appropriate root of (18) and $\rho_1^{(2)}$ evaluated by computer simulations are shown in Fig. 1. From the second equation in (8) at $\beta_2^* = \alpha_2^*$

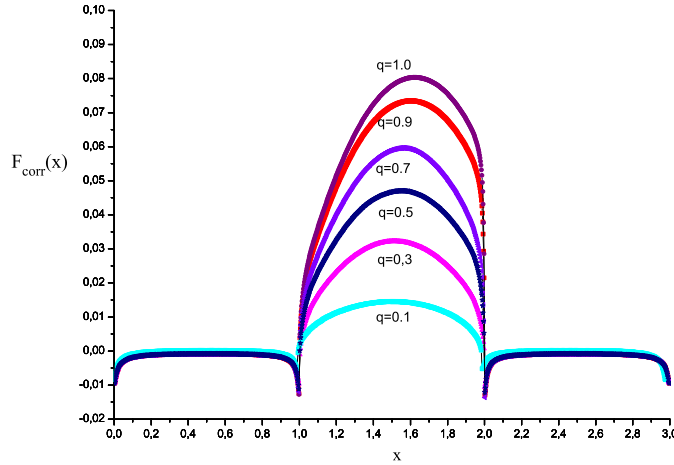


FIG. 3. (Color online) Position dependence of the nearest-neighbor correlations along the network at different values of q . The normalized coordinate $x = i/L$ is the same as in Fig. 2.

we have $\alpha_3^* = 1/(4\alpha_2^*)$, so that $\alpha_2^* < 1/2$ directly implies $\alpha_3^* > 1/2$.

Predictions of the domain wall theory. — An open chain with stationary current $J < 1/4$ in the thermodynamic limit can be found in two phases: with low density $\rho_-(J)$ and high density $\rho_+(J)$. According to the domain wall theory [15], on the coexistence line the two phases are separated by a completely delocalized domain wall. As a result, the averaged density profile is linear, changing its value from $\rho_-(J)$ at the left end of the chain to $\rho_+(J)$ at its right end. This prediction is compared to numerical simulation data in Fig. 2 for external rates $\alpha = \beta = 0.75$, length of each segment $L = 400$, and $q = 0.5$. The data was averaged over 100 runs of length 2^{23} attempted moves each. One sees a very good agreement between the theoretical prediction $\rho_1^{(2)} = \rho_-(J^{(2)}) \simeq 0.282$ and the simulation result $\rho_1^{(2)} \simeq 0.286$. Fairly good is also the agreement at the high-density end, between the theoretical prediction $\rho_{400}^{(2)} = \rho_+(J^{(2)}) \simeq 0.718$ and the simulation result $\rho_{400}^{(2)} \simeq 0.701$.

Another important prediction of the domain wall theory is the parabolic shape of the nearest-neighbor correlations $F_{\text{cor}}(x) = \langle \tau_i^{(2)} \tau_{i+1}^{(2)} \rangle - \langle \tau_i^{(2)} \rangle \langle \tau_{i+1}^{(2)} \rangle$ as a function of the normalized distance $x = i/L$. The simulation results for all q show almost vanishing correlations in the bulk of the first and third segments and a parabolic-like shape in the second segment, see Fig. 3. In the latter case the noticeable tilt of the 'parabolas' to the right when $q \geq 0.7$ may be due to the different value of the correlations $G^{(s,s+1)}$ between the segments s and

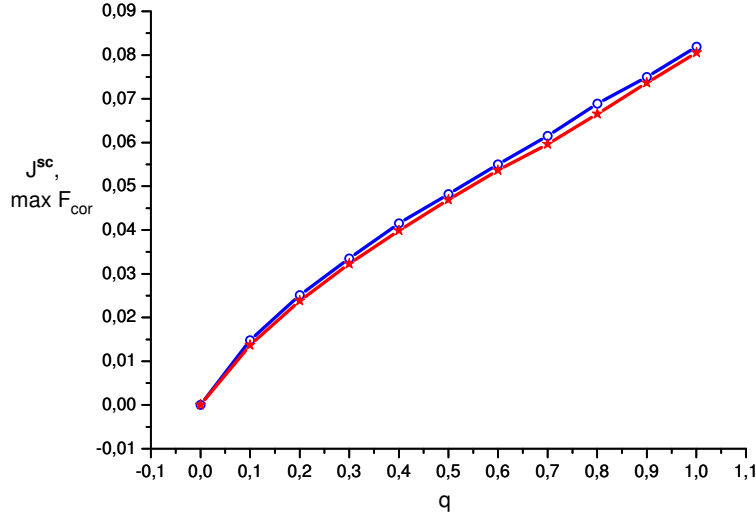


FIG. 4. (Color online) Comparison between the numerically estimated maximum value of the nearest-neighbor correlations in the second segment $\max_x F_{\text{cor}}(x)$, shown by red stars connected with a red line, and the current J^{sc} through the shortcut, shown by blue circles connected with a blue line, at different values of the parameter q .

$s+1$, $s = 1, 2$. For example, we have numerically evaluated $G^{(1,2)} \simeq -0.0073$ at both $q = 0.3$ and $q = 1.0$, while $G^{(2,3)} \simeq -0.0023$ at $q = 0.3$ but $G^{(2,3)} \simeq 0.0095$ at $q = 1.0$. Theoretically, the maximum value of $F_{\text{cor}}(x)$ is reached at the midpoint of the chain and equals

$$\max_x F_{\text{cor}}(x) = [\rho_+(J^{(2)}) - \rho_-(J^{(2)})]^2/4 = 1/4 - J^{(2)} = J^{\text{sc}}.$$

The validity of this prediction of the domain wall theory is illustrated in Fig. 4.

Conclusions. — The model predicts that a shortcut in the bulk of a road carrying maximum stationary current inevitably causes traffic jams characteristic of a shock phase with completely delocalized domain wall. The main parameters of the average density profile and the nearest-neighbor correlations in the shunted segment are governed by a cubic equation with coefficients simply depending on the probability of choosing the shortcut.

Acknowledgements. — N.B. gratefully acknowledges support from a grant of the Representative Plenipotentiary of Bulgaria to the Joint Institute for Nuclear Research in Dubna. N.P. thanks Roumen Anguelov and Jean Lubuma for their hospitality at the University of

Pretoria, where a part of this work was also carried out.

-
- [1] C. T. MacDonald, J. H. Gibbs, and A. C. Pipkin, *Biopolymers* **6**, 1 (1968).
 - [2] K. Nagel, M. Schreckenberg, *J. Physique I* **2**, 2221 (1992); D. Chowdhury, L. Santen, and A. Schadschneider, *Phys. Rep.* **329**, 199 (2000); D. Helbing, *Rev. Mod. Phys.* **73**, 1067 (2001).
 - [3] A. Parmeggiani, T. Franosch, and E. Frey, *Phys. Rev. Lett.* **90**, 086601 (2003); A. Roux, G. Capello, J. Cartaud, J. Prost, B. Goud, and P. Bassereau, *Proc. Natl. Acad. Sci. USA* **99**, 5394 (2002); G. Koster, M. VanDuijn, B. Hofs, and M. Dogterom, *Proc. Natl. Acad. Sci. USA* **100**, 15583 (2003); T. M. Nieuwenhuizen, S. Klumpp, and R. Lipowsky, *Phys. Rev. E* **69**, 061911 (2004); C. Leduc, O. Campas, K. B. Zeldovich, A. Roux, P. Jolimaître, L. Bourel-Bonnet, B. Goud, J.-F. Joanny, P. Bassereau, and J. Prost, *Proc. Natl. Acad. Sci. USA* **101**, 17096 (2004); C. Leduc, K. Padberg-Gehle, V. Varga, D. Helbing, S. Diez, and J. Howard, *PNAS* **109**, 6100 (2013); I. Neri, N. Kern, and A. Parmeggiani, *Phys. Rev. Lett.* **110**, 098102 (2013).
 - [4] J. Krug and H. Spohn, *Phys. Rev. A* **38**, 4271 (1988); J. Krug, P. Meakin, and T. Halpin-Healy, *Phys. Rev. A* **45**, 638 (1992); T. Sasamoto, *J. Phys. A* **38**, L549 (2005).
 - [5] T. Chou and D. Loshe, *Phys. Rev. Lett.* **82**, 3552 (1999); Q.-H. Wei, C. Bechinger, and P. Leiderer, *Science* **287**, 625 (2000); A. B. Kolomeisky, *Phys. Rev. Lett.* **98**, 048105 (2007).
 - [6] T. Huisinga, R. Barlovic, W. Knopse, A. Schadschneider, M. Schreckenberg, *Physica A* **294**, 249 (2001).
 - [7] T. Reichenbach, E. Frey, and T. Franosch, *New J. Phys.* **9**, 159 (2007).
 - [8] T. Karzig and F. von Oppen, *Phys. Rev. B* **81**, 045317 (2010).
 - [9] J. Brankov, N. Pesheva, and N. Bunzarova, *Phys. Rev. E* **69**, 066128 (2004).
 - [10] E. Pronina, A. B. Kolomeisky, *J. Stat. Mech.: Theory Exp.*, P07010 (2005).
 - [11] P. Pierobon, M. Mobilia, R. Kouyos, and E. Frey, *Phys. Rev. E* **74**, 031906 (2006); Z.-P. Cai, Y.-M. Yang, R. Jiang, M.-B. Hu, Q.-S. Wu, and Y.-H. Wu *J. Stat. Mech.: Theor. Exp.*, P07016 (2008); B. Embley, A. Parmeggiani, N. Kern, *J. Phys.: Condens. Matter* **20**, 295213 (2008); Z.-P. Cai, Y.-M. Yuan, R. Jiang, K. Nishinary and Q.-S. Wu - *J. Stat. Mech.: Theor. Exp.*, P02050 (2009); X. Wang, R. Jiang, K. Nishinary, M.-B. Hu, and Q.-S. Wu - *Int. J. Mod. Phys. C* **20**, 967 (2009); X. Wang, R. Jiang, M.-B. Hu, K. Nishinary, and Q.-S. Wu - *Int. J. Mod. Phys. C* **20**, 1999 (2009); B. Embley, A. Parmeggiani, N. Kern, *Phys. Rev. E* **80**, 041128 (2009).

- (2009); H.-F. Du, Y.-M. Yuan, M.-B. Hu, R. Wang, R. Jiang and Q.-S. Wu, J. Stat. Mech.: Theor. Exp., P03014 (2010); I. Neri, N. Kern, and A. Parmeggiani, Phys. Rev. Lett. **107**, 068702 (2011); X. Song, L. Ming-Zhe, W. Jian-Jun, and W. Hua, Chin. Phys. B **20**, 060509 (2011); S. Xia, L. Tang, H. Wang, Cent. Eur. J. Phys., **9**, 1077 (2011); C. Appert-Rolland, J. Cividini and H. J. Hilhorst - J. Stat. Mech., P10014 (2011); R. Chatterjee, A. K. Chandra, and A. Basu, Phys. Rev. E **87**, 032157 (2013); A. Raguin, A. Parmeggiani, and N. Kern, Phys. Rev. E **88**, 042104 (2013).
- [12] N. C. Pesheva and J. G. Brankov, Phys. Rev. E **87**, 062116 (2013).
- [13] Y.-M. Yuan, R. Jiang, R. Wang, M.-B. Hu, and Q.-S. Wu, J. Phys. A **40**, 12351 (2007).
- [14] B. Derrida, E. Domany, and D. Mukamel, J. Stat. Phys. **69**, 667 (1992); B. Derrida, M. R. Evans, V. Hakim and V. Pasquier, J. Phys. A: Math. Gen. **26**, 1493 (1993).
- [15] A. B. Kolomeisky, G. M. Schütz, E. B. Kolomeisky and J. P. Straley, J. Phys. A **31**, 6911 (1998); L. Santen and C. Appert, J. Stat. Phys. **106**, 187 (2002).